Acute Geometric Changes of the Mitral Annulus after Coronary Occlusion: A Real-Time 3D Echocardiographic Study

We performed real-time 3D echocardiography in sixteen sheep to compare acute geometric changes in the mitral annulus after left anterior descending coronary artery (LAD, n=8) ligation and those after left circumflex coronary artery (LCX, n=8) ligation. The mitral regurgitation (MR) was quantified by regurgitant volume (RV) using the proximal isovelocity surface area method. The mitral annulus was reconstructed through the hinge points of the annulus traced on 9 rotational apical planes (angle increment=20°). Mitral annular area (MAA) and the ratio of antero-posterior (AP) to commissure-commissure (CC) dimension of the annulus were calculated. Non-planar angle (NPA) representing non-planarity of the annulus was measured. After LCX occlusion, there were significant increases of the MAA during both early and late systole ($p<0.01$) with significant MR (RV: 30 ± 14 mL), while there was neither a significant increase of MAA, nor a significant MR (RV: 4 ± 5 mL) after LAD occlusion. AP/CC ratio ($p<0.01$) and NPA ($p<0.01$) also significantly increased after LCX occlusion during both early and late systole. The mitral annulus was significantly enlarged in the antero-posterior direction with significant decrease of non-planarity compared to LAD occlusion immediately after LCX occlusion.

Key Words : *Mitral Valve; Mitral Annulus; Echocardiography; Coronary Disease*

Jun Kwan, Beom Woo Yeom*,
Michael Jones[†], Jian Xin Qin[†],
Arthur D. Zetts[‡], James D. Thomas[†],
Takahiro Shiota[†]

Department of Cardiology, Inha University Hospital, Inchon; Department of Pathology*, Korea University College of Medicine, Seoul, Korea; [†]Cardiovascular Imaging Center, Department of Cardiology, The Cleveland Clinic Foundation, Cleveland, Ohio; [‡]National Heart, Lung and Blood Institute, Bethesda, Maryland, U.S.A.

Address for correspondence
Jun Kwan, M.D.
Department of Cardiology, Inha University Hospital, 7-206 3-ga, Shinheung-dong, Jung-gu, Inchon 400-711, Korea
Tel : +82.32-890-2453, Fax : +82.32-890-2447
E-mail : kuonmd@inha.ac.kr

INTRODUCTION

Mitral annular dilatation has been regarded as one of important geometric factors causing ischemic mitral regurgitation (MR) (1). Accordingly, the reduction of annular size by annuloplasty has been the conventional surgical treatment for ischemic MR (2-5). Several studies have demonstrated annular dilatation after left circumflex artery (LCX) occlusion (6, 7). With the use of 3D imaging techniques, the appreciation of the non-planar geometry of the mitral annulus and its accurate measurement has been achieved (8, 9). Several previous studies by fluoroscopy of radiopaque markers or transesophageal echocardiography with a rotating transducer have revealed dilatation of the mitral annulus after LCX occlusion (10-13). However, acute geometric alterations including non-planarity of the mitral annulus after LCX occlusion compared to left anterior descending artery (LAD) occlusion have not been described in detail. Real-time 3 dimensional echocardiography (RT3DE) has been validated for its quantitative accuracy of geometric measurement of cardiac structures (14).

The present study, therefore, was conducted to detail and to compare the geometric changes in the mitral annulus immediately after LAD and LCX occlusion using RT3DE.

MATERIALS AND METHODS

Surgical preparation

Sixteen juvenile sheep weighing 43 ± 8 kg (range 28 to 56) were studied. All of them had pre-existing apical aneurysm developed by chronic ligation of the distal LAD. The mid portion of LAD was ligated in 8 sheep and the proximal LCX in the other 8 sheep.

During the acquisition of volumetric images using RT3DE, the sheep were anesthetized with intravenous sodium pentobarbital (25 mg/kg) and maintained with 1-2% isoflurane with oxygen. The animals were ventilated via an endotracheal tube using a volume-cycled ventilator. A median sternotomy was performed. Bleeding, insensible fluid loss and associated electrolyte disturbances were monitored frequently and corrected by continuous infusion of lactated Ringer's solution and 5% dextrose in water supplemented with potassium, if necessary. All operative and animal management procedures were approved by the Animal Care and Use Committee of the National Heart, Lung and Blood Institute (15).

Volumetric image acquisition using real-time 3D echocardiography

A RT3DE imaging system with a 2.5 or 3.5 MHz hand held transducer was used to image the mitral annulus (Volumetric Medical Imaging Inc., Durham, NC, U.S.A.). The volumetric frame rate was 17-22 volumes/second with an imaging depth of 12-16 cm. For all subjects, volumetric images were obtained epicardially using the apical view before and after the coronary occlusion. For comparison of the geometric changes in the mitral annulus, we acquired images at specific phases of the cardiac cycle: in early systole/the image of the frame immediately after the closure of the mitral valve, and in late systole/the image of the frame just before the mitral valve opening. Care was taken to include the entire mitral annulus in the volumetric data set during each cardiac cycle. All volumetric images were digitally stored on magnetic optical disks for off-line analysis.

3D reconstruction of the mitral annulus

Volumetric data were digitally transferred to a PC in which the 3D data were segmented into 9 rotational apical planes (angle increment=20°) around the rotational axis from the left ventrical (LV) apex through the center of the mitral annulus (Fig. 1) using commercially available software (3D Echo-Tech, Lafayette, Co., U.S.A.). A series of digital still images were generated and imported into a custom software package programmed in our laboratory in the LabVIEW environment (National Instruments, Austin, TX, U.S.A.). The mitral leaflet hinge points in each plane were identified during early and late systole. All these locations were converted into a Cartesian coordinate system with x, y and z axes. The mitral annulus was then reconstructed from fitting, interpolation and Fourier transformation.

2D echocardiography

For all subjects, 2D echocardiography (Toshiba Co., Tokyo, Japan) was done before and after coronary occlusion. LV end-diastolic volumes (EDV), end-systolic volumes (ESV) and ejection fractions (EF) were measured by the biapical planes Simpson disk method (16). For quantification of the severity of mitral regurgitation (MR), regurgitant volumes (RV) were calculated using the proximal isovelocity surface area (PISA) method (17).

Measurements of Mitral annular perimeter (MAP) and area (MAA)

The hinge points of the mitral annulus traced on each rotating apical plane were transformed into a common 3D coordinate system. To fit a smooth curve representing the mitral annulus, Fourier series approximations in each of the spatial coordinates (x, y, z) were constructed. The 3D mitral annular perimeter (MAP) was automatically calculated from those fitted data. The mitral annular area (MAA) was computed as the area projected onto the least-squares plane fitted to the annular curve.

Commissure-commissure and antero-posterior dimension

Using the TomTec system (Echoscan, TomTec, Boulder, Co., Germany), an apical, commissure to commissure (CC)
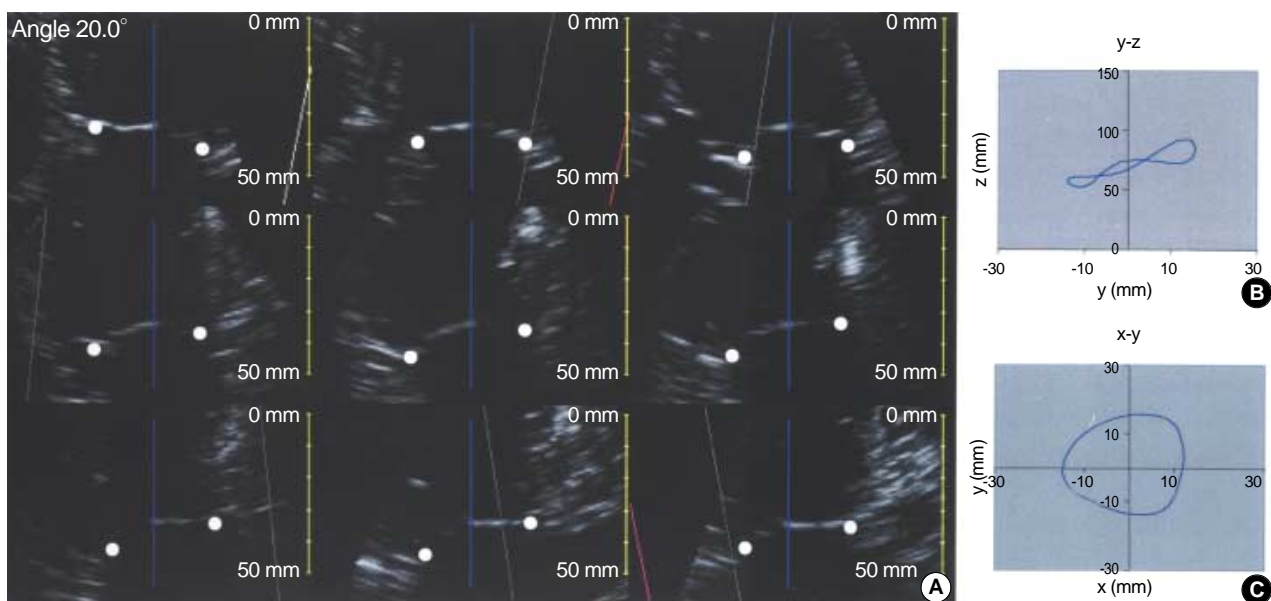

Fig. 1. Nine rotational apical planes were used to trace 18 hinge points (white dots) of the mitral annulus (A). 3D shape of the mitral annulus reconstructed from the 18 hinge points (B). Projected view of 3D reconstructed annulus (C).

plane crossing two commissures on the cross-sectional plane at the level of the mitral valve, simultaneously viewed from LV, was obtained. Another orthogonal plane, antero-posterior (AP) perpendicularly crossing the center of the commissure to commissure axis was acquired (Fig. 2). CC and the AP dimensions defined by the distances between the two hinge points of the annulus on those two planes were then measured during early and late systole.

For estimation of circularization of the mitral annulus associated with its dilatation, the ratio of these two dimensions (AP/CC dimension) were calculated.

Non-planarity

According to several previous reports defining the shape of the mitral annulus as "saddle" shaped with two cephalad portions at the anteroseptal and posterior portions of the annulus (18, 19), we assumed that the mid portion of the anterior and the posterior annulus would be the most cephalad portion of each annulus. For evaluation of the non-planarity of the "saddle" shaped mitral annulus, the non-planar angle (NPA), the angle between the two vectors from the two hinge points of the annulus in the AP plane to the center of the CC axis was measured using 3D computer software (TomTec, Co.) (Fig. 2).

Statistic analysis

Data are expressed as mean $\pm$ SD. The fractional change of the measurements was defined as the percentage change
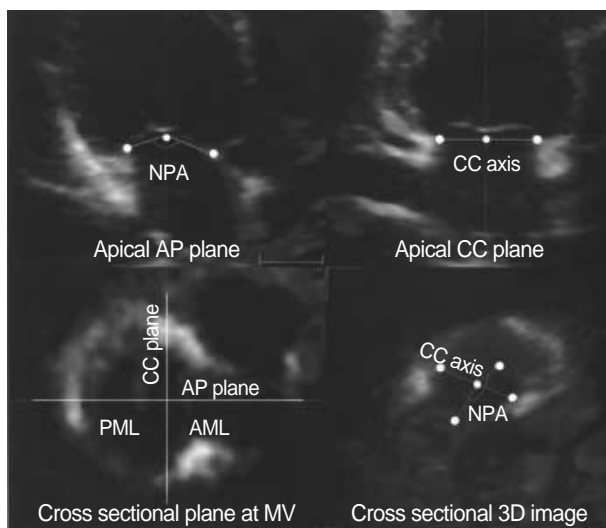

Fig. 2. Volumetric image showing how the non-planar angle (NPA) of the annulus was measured. Using 3D computer software (TomTec), we measured the angle between two vectors from two hinge points of the annulus (white dots) in the antero-posterior (AP) plane to the center of the axis connecting two commssures (white dot) in the commissure-commissure (CC) plane. AML, anterior mitral leaflet; MV, mitral valve; PML, posterior mitral leaflet.

of the measurements from early to late systole. Student's t-test was used to compare all data between the two groups, before and after coronary occlusion. The relationship between two parameters was evaluated by linear regression analysis. A value of $p<0.05$ was considered to be significant.

RESULTS

2D echocardiographic measurements

Before coronary occlusion, there was no significant difference of LV volumes (EDV: 75 ± 25 vs. 76 ± 23 mL, ESV: 49 ± 25 vs. 50 ± 23 mL, $p>0.05$) and global LV systolic function (EF: 36 ± 17 vs. $36\pm14\%$, $p>0.05$) between the LAD and LCX groups. After coronary occlusion, there were statistically insignificant increases of LV volume in the both LAD (EDV: 92 ± 29 mL, ESV: 73 ± 28 mL, $p>0.05$) and LCX groups (EDV: 92 ± 25 mL, ESV: 74 ± 23 mL, $p>0.05$), but significant decreases of global LV systolic function (EF) in both groups to $23\pm6\%$ and $20\pm6\%$ ($p<0.05$). Before coronary occlusion there was no significant MR in either the LAD or the LCX group. After coronary occlusion, all subjects in the LCX group developed substantial MR with RV of 30 ± 14 mL, while no subjects developed significant MR in the LAD group with RV of 4 ± 5 mL.

Geometric changes in the mitral annulus

Changes of all measurements of the mitral annulus in both two groups after coronary occlusion are shown in Table 1. There was no significant difference in all the mitral annular measurements between the LAD and LCX groups before coronary occlusion. After LAD occlusion, no significant

Table 1. Geometric measurements of the mitral annulus

	Pre-occlusion		Post-occlusion	
	LAD	LCX	LAD	LCX
Early systole				
MAP (cm)	9.0 ± 0.3	8.7 ± 0.3	9.4 ± 0.3	$9.7\pm0.6^*$
MAA (cm²)	6.3 ± 0.5	6.2 ± 0.4	6.8 ± 0.4	$7.4\pm0.7^*$
CC (cm)	3.0 ± 0.1	2.9 ± 0.1	3.1 ± 0.1	3.0 ± 0.1
AP (cm)	2.5 ± 0.04	2.4 ± 0.1	2.6 ± 0.1	$2.9\pm0.2^*$
AP/CC	0.84 ± 0.02	0.83 ± 0.04	0.86 ± 0.03	$0.97\pm0.04^*$
NPA (°)	128 ± 5	128 ± 6	131 ± 5	$137\pm4^*$
Late Systole				
MAP (cm)	9.2 ± 0.2	9.0 ± 0.3	9.6 ± 0.3	$9.9\pm0.5^*$
MAA (cm²)	6.5 ± 0.3	6.4 ± 0.4	6.9 ± 0.4	$7.6\pm0.7^*$
CC(cm)	3.0 ± 0.1	2.9 ± 0.1	3.1 ± 0.1	3.0 ± 0.1
AP(cm)	2.6 ± 0.1	2.6 ± 0.1	2.7 ± 0.1	$3.0\pm0.2^*$
AP/CC	0.87 ± 0.03	0.87 ± 0.04	0.89 ± 0.02	$0.99\pm0.02^*$
NPA (°)	137 ± 3	138 ± 4	140 ± 4	142 ± 4

AP, antero-posterior dimension; CC, commissure-commissure dimension; MAA, mitral annular area; MAP, mitral annular perimeter; NPA, non-planar angle. *$p<0.01$ vs. pre-occlusion.

changes in MAP, MAA, CC dimension or AP dimension were observed during early and late systole. However, after LCX occlusion, there were significant increases in all of these measurements except for the CC dimension. The ratio of AP to CC dimension, reflecting the degree of circularization of the mitral annulus, significantly increased from 0.83 ± 0.04 to 0.97 ± 0.04 ($p<0.01$) during early systole and from 0.87 ± 0.04 to 0.99 ± 0.02 ($p<0.01$) during late systole after LCX occlusion, while it showed no significant change after LAD occlusion (Table 1).

NPA, representing the non-planarity of the mitral annulus, showed no significant change after LAD occlusion dur-

ing early ($128 \pm 5°$ vs. $131 \pm 5°$, $p>0.05$) and late ($137 \pm 3°$ vs. $140 \pm 4°$, $p>0.05$) systole. After LCX occlusion, there was a significant increase in NPA during early systole ($128 \pm 6°$ vs. $137 \pm 4°$, $p<0.01$), but an insignificant increase during late systole ($138 \pm 4°$ vs. $142 \pm 4°$, $p>0.05$) (Fig. 3) resulting in a significant decrease inthe fractional change of NPA during systole (Table 2).

Relationships between the changes of geometric measurements

In the LCX group, the percentage changes ($\triangle$) in the geometric measurements after coronary occlusion were calculated: $\triangle$NPA showed significant positive correlations ($p<0.01$) with $\triangle$MAA and $\triangle$AP dimension during both early (r=0.78, r=0.89) and late systole (r=0.82, r=0.84) (Fig. 4). However, $\triangle$MAA and $\triangle$NPA during late systole showed a weak but statistically insignificant relationship with RV, the degree of MR (r=0.56, r=0.53, $p>0.05$) (Fig. 5).

Table 2. Fractional changes of annular measurements during systole

	Pre-occlusion		Post-occlusion	
	LAD	LCX	LAD	LCX
MAA (%)	2.2 ± 2.7	3.0 ± 2.1	2.1 ± 3.8	1.2 ± 2.3
CC (%)	1.3 ± 1.5	1.4 ± 1.0	1.3 ± 1.7	0.9 ± 1.7
AP (%)	4.2 ± 1.7	6.0 ± 1.5	5.1 ± 1.0	$3.5 \pm 1.1^*$
NPA (%)	6.7 ± 2.0	7.4 ± 1.7	6.6 ± 2.1	$3.9 \pm 1.2^*$

AP, antero-posterior dimension; CC, commissure-commissure dimension; MAA, mitral annular area; NPA, non-planar angle.
*$p<0.01$ vs. pre-occlusion.

DISCUSSION

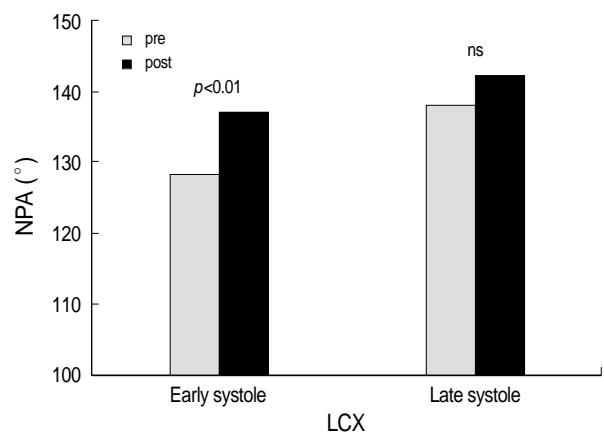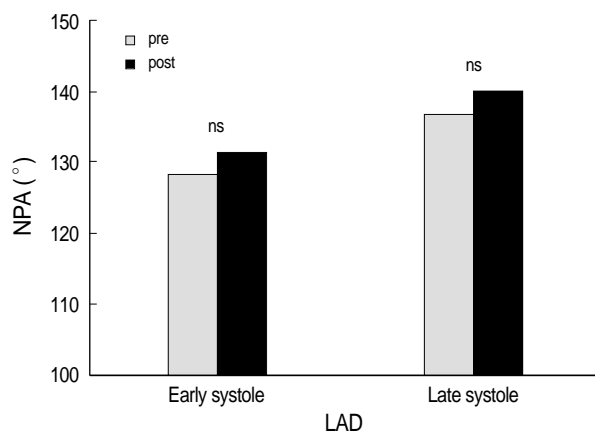Three dimensional reconstruction of the mitral annulus

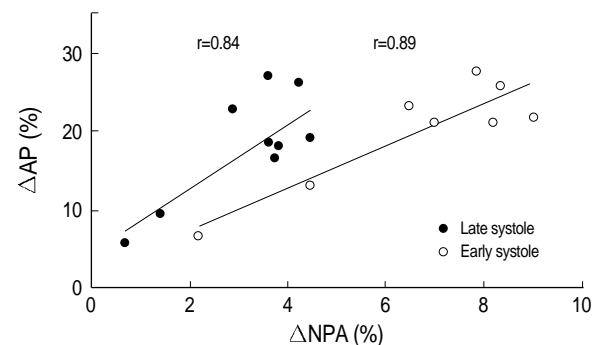Fig. 3. Change of the non-planar angle (NPA) of the mitral annulus after coronary occlusion.
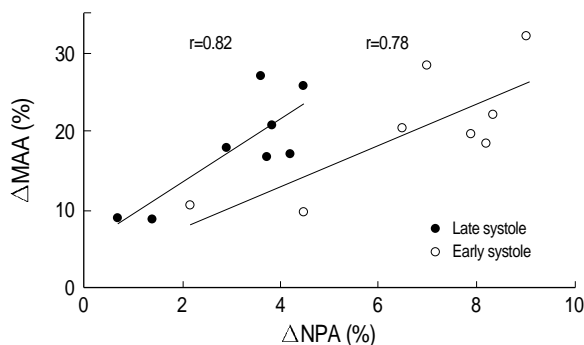

Fig. 4. Graphs showing significant correlations ($p<0.01$) of percent change ($\triangle$) of the non-planar angle (NPA) with that of the mitral annular area (MAA) and the antero-posterior dimension (AP).
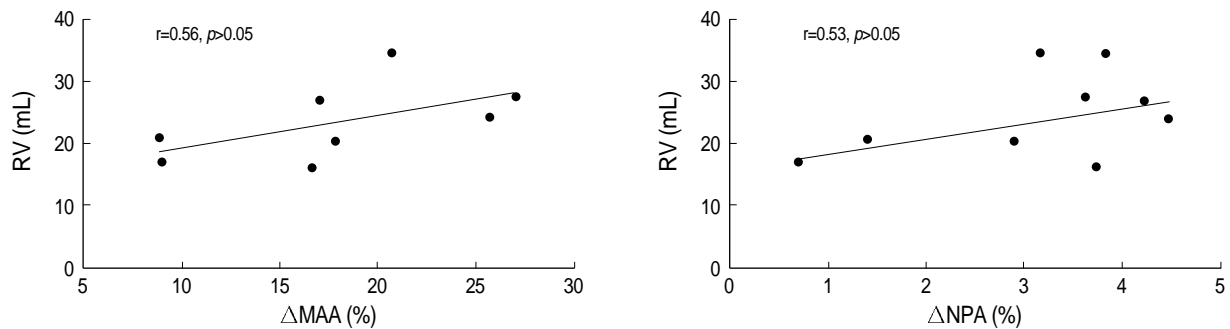
Fig. 5. Graphs showing weak but statistically insignificant correlations (p>0.05) of percent change (△) of the mitral annular area (MAA) and the non-planar angle (NPA) with regurgitant volume (RV).
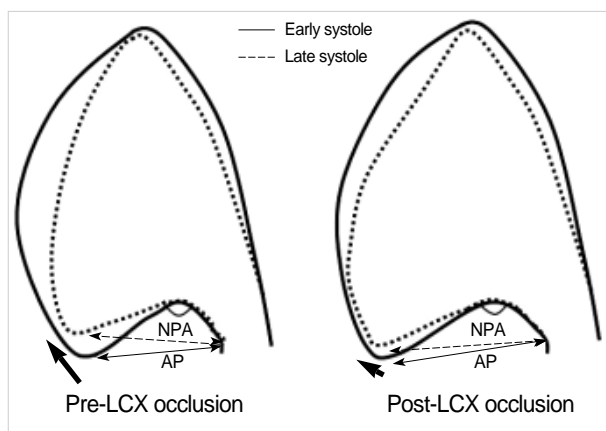

Fig. 6. Apical movement of the posterior annulus (arrow) before and after LCX occlusion. AP, antero-posterior dimension; NPA, non-planar angle. Note the smaller movement of the posterior annulus after LCX occlusion than before the occlusion.

by fitting, interpolation and Fourier transformation of 3D volumetric data enabled us to image the 3D shape of annulus before and after coronary occlusion.

Previous echocardiographic studies have utilized rotational acquisition of apical views using either transthoracic or transesophageal probes to measure or to reconstruct the mitral annulus. These methods required ECG and respiratory gating over multiple cardiac cycles to collect the 3D data sets. MRI also has been used for analyzing mitral annular geometry. Despite its high spatial resolution, it is limited with lengthy acquisition time and poor temporal resolution. To the contrary, RT3DE does not require ECG or respiratory gating for acquisition of 3D volumetric data. The data are obtained by electronic scanning of the ultrasound beam in three dimensions with temporal resolution of about 50 msec (20 Hz). In addition, we could eliminate errors in measuring annular parameters by reconstructing the shape of the annulus using a Fourier fitting model instead of the original raw data.

The mitral annulus consists of two components, an anterior fibrous component and a posterior muscular component. According to the current study, there was enlargement (18-20%) and circularization of the mitral annulus after LCX occlusion compared to LAD occlusion. This probably resulted

from the annular dilatation being confined to the posterior part of annulus, the muscular component, which was affected by the posterior wall infarction caused by LCX occlusion. This finding is consistent with the observations from previous animal studies (6, 20). Glasson et al. (6) suggested that the enlargement and subsequent circularization of the mitral annulus might augment the extent of incomplete leaflet closure. However, considering that the valve tolerance to annular dilatation in normal papillary muscle position was 1.8-2.0 times normal (21-25), an annular enlargement of 18-20% might not be enough to produce incomplete leaflet closure causing significant MR. Moreover, we observed weak relationships between the geometric changes of the mitral annulus and MR severity even though, the number of the population in the present study was too small (n=8) to interpret them with statistical significance. On the other hand, the annular size has been reported to be related to MR severity. in several previous studies (26, 27). The inconsistency might be resulted from that the populations of those studies usually consisted of patients with chronic functional MR, in whom the annulus were chronically enlarged probably in excess of 18-20%. Nevertheless, MV tenting area defined mainly by leaflet tethering was suggested as the strongest determinant of MR severity rather than the annular size by multivariate regression analysis in those studies. Therefore, an annular enlargement of 18-20% alone immediately after LCX occlusion does not seem to play a primary role in generating enough incomplete leaflet closure to cause substantial MR. Instead, it may play an augmentative role to other geometric changes such as leaflet tethering by displaced papillary muscles, as has been suggested as a main cause for ischemic MR (12, 13).

Non-planarity of the mitral annulus has been assessed by other 3D echocardiographic studies (18, 28). In the present study, we estimated non-planarity of the mitral annulus by measuring the angle between two vectors from two hinge points of the annulus in the antero-posterior plane to the center of the commissure to commissure axis on the assumption that two most cephalad portion of the annulus would be located at the mid portion of the annulus. We observed that the non-planarity of the mitral annulus significantly decreased after LCX occlusion compared to LAD occlusion,

especially during early systole with subsequent reduction of its fractional change during systole. The degree of change in the NPA after LCX occlusion showed a good relationship with that of annular size in the antero-posterior direction. The reduction of the fractional change in the NPA during systole after LCX occlusion might have resulted from decreased apical movement of the posterior annulus due to impaired contractility of the infarcted posterior myocardium (Fig. 6) as suggested in the previous study (29).

In the present study there were several limitations. Firstly, we did not estimate mitral regurgitant volume by electro-magnetic flow probes but by the PISA method, because of the concern that the geometry of the mitral annulus would be affected by the implanted electromagnetic flow probe. In addition, good relationships between the degree of MR esti-mated by PISA and that by electromagnetic flow probe has been previously demonstrated (30, 31).

Secondly, compared with conventional 2D images, the spatial resolution of the volumetric images is limited due to the frequency of the transducer. However, the mitral annu-lar hinge points have strong signal intensities, which make it relatively easy to identify them. In the present study, we defined two specific phases, early and late systole, not by ECG but by valvular motion. Nevertheless, there may be image/phases mismatches because of the low frame rates of 20 frame/sec.

Finally population number was too small to explore the geometric factor determining of MR severity immediately after coronary arterial occlusion. In addition, the change in the annular geometry was not explored in association with the degree of the papillary muscle displacement which can be as a determinant of ischemic MR.

According to the results of the present study, the mitral annulus was significantly enlarged and circularized imme-diately after LCX occlusion compared to LAD occlusion. And the non-planarity of the annulus significantly decreased, espe-cially during early systole, after LCX occlusion with conse-quent reduction of its fractional change during systole.

REFERENCES

1. Gahl K, Sutton R, Pearson M, Caspari P, Lairet A, McDonald L. *Mitral regurgitation in coronary heart disease. Br Heart J 1977; 39: 13-8.*

2. Hendren WG, Nemec JJ, Lytle BW, Loop FD, Taylor PC, Stewart RW, Cosgrove DM 3rd. *Mitral valve repair for ischemic mitral insuf-ficiency. Ann Thorac Surg 1991; 52: 1246-51.*

3. Czer LS, Maurer G, Trento A, DeRobertis M, Nessim S, Blanche C, Kass RM, Chaux A, Matloff JM. *Comparative efficacy of ring and suture annuloplasty for ischemic mitral regurgitation. Circulation 1992; 86: 46-52.*

4. Dion R. *Ischemic mitral regurgitation: When and how should it be corrected? J Heart Valve Dis 1993; 2: 536-43.*

5. Timek T, Glasson JR, Dagum P, Green GR, Nistal JF, Komeda M, Daughters GT, Bolger AF, Foppiano LE, Ingels NB Jr, Miller DC. *Ring annuloplasty prevents delayed leaflet coaptation and mitral regurgitation during acute left ventricular ischemia. J Thorac Car-diovasc Surg 2000; 119: 774-83.*

6. Glasson JR, Komeda M, Daughters GT, Bolger AF, Karlsson MO, Foppiano LE, Hayase M, Oesterle SN, Ingels NB Jr, Miller DC. *Early systolic mitral leaflet ''loitering'' during acute ischemic mitral regur-gitation. J Thorac Cardiovasc Surg 1998; 116: 193-205.*

7. Gorman JH 3rd, Gorman RC, Jackson BM, Hiramatsu Y, Gikakis N, Kelley ST, Sutton MG, Plappert T, Edmunds LH Jr. *Distortions of the mitral valve in acute ischemic mitral regurgitation. Ann Tho-rac Surg 1997; 64: 1026-31.*

8. Levine RA, Handschumacher MD, Sanfilippo AJ, Hagege AA, Har-rigan P, Marshall JE, Weyman AE. *Three-dimensional echocardio-graphic reconstruction of the mitral valve, with implications for the diagnosis of mitral valve prolapse. Circulation 1989; 80: 589-98.*

9. Salustri A, Becker AE, van Herwerden L, Vletter WB, Ten Cate FJ, Roelandt JR. *Three-dimensional echocardiography of the normal and pathologic mitral valve: a comparison with two-dimensional transesophageal echocardiography. J Am Coll Cardiol 1996; 27: 1502-10.*

10. Glasson JR, Komeda M, Daughters GT 2nd, Bolger AF, MacIsaac A, Oesterle SN, Ingels NB Jr, Miller DC. *Three-dimensional dynam-ics of the canine mitral annulus during ischemic mitral regurgitation. Ann Thorac Surg 1996; 62: 1059-67.*

11. Komeda M, Glasson JR, Bolger AF, Daughters GT 2nd, MacIsaac A, Oesterle SN, Ingels NB Jr, Miller DC. *Geometric determinants of ischemic mitral regurgitation. Circulation 1997; 96: 128-33.*

12. Dagum P, Timek TA, Green GR, Lai D, Daughters GT, Liang DH, Hayase M, Ingels NB Jr, Miller DC. *Coordinate-free analysis of mitral valve dynamics in normal and ischemic hearts. Circulation 2000; 102: 62-9.*

13. Otsuji Y, Handschumacher MD, Liel-Cohen N, Tanabe H, Jiang L, Schwammenthal E, Guerrero JL, Nicholls LA, Vlahakes GJ, Levine RA. *Mechanism of ischemic mitral regurgitation with segmental left ventricular dysfunction: three-dimensional echocardiographic stud-ies in models of acute and chronic progressive regurgitation. J Am Coll Cardiol 2001; 37: 641-8.*

14. Binder TM, Rosenhek R, Porenta G, Maurer G, Baumgartner H. *Improved assessment of mitral valve stenosis by volumetric real-time three-dimensional echocardiography. J Am Coll Cardiol 2000; 36: 1355-61.*

15. Shiota T, Jones M, Chikada M, Fleishman CE, Castellucci JB, Cotter B, DeMaria AN, von Ramm OT, Kisslo J, Ryan T, Sahn DJ. *Real-time three-dimensional echocardiography for determining right ven-tricular stroke volume in an animal model of chronic right ventricu-lar volume overload. Circulation 1998; 97: 1897-900.*

16. Schiller NB, Shah PM, Crawford M, DeMaria A, Devereux R, Fei-genbaum H, Gutgesell H, Reichek N, Sahn D, Schnittger I, Silverman NH, Tajik AJ. *Recommendations for quantitation of the left ventricle by two-dimensional echocardiography. American Society of Echo-cardiography Committee on Standards, Subcommittee on Quantitation of Two-dimensional Echocardiograms. J Am Soc Echocardiogr 1989;*

2: 358-67.

17. Aotsuka H, Tobita K, Hamada H, Uchishiba M, Tateno S, Matsuo K, Fujiwara T, Niwa K. *Validation of the proximal isovelocity surface area method for assessing mitral regurgitation in children. Pediatr Cardiol 1996; 17: 351-9.*

18. Flachskampf FA, Chandra S, Gaddipatti A, Levine RA, Weyman AE, Ameling W, Hanrath P, Thomas JD. *Analysis of shape and motion of the mitral annulus in subjects with and without cardiomyopathy by echocardiographic 3-dimensional reconstruction. J Am Soc Echocardiogr 2000; 13: 277-87.*

19. Pai RG, Tanimoto M, Jintapakorn W, Azevedo J, Pandian NG, Shah PM. *Volume-rendered three-dimensional dynamic anatomy of the mitral annulus using a transesophageal echocardiographic technique. J Heart Valve Dis 1995; 4: 623-7.*

20. Gorman RC, McCaughan JS, Ratcliffe MB, Gupta KB, Streicher JT, Ferrari VA, St John-Sutton MG, Bogen DK, Edmunds LH Jr. *Pathogenesis of acute ischemic mitral regurgitation in three dimensions. J Thorac Cardiovasc Surg 1995; 109: 684-93.*

21. Boltwood CM, Tei C, Wong M, Shah PM. *Quantitative echocardiography of the mitral complex in dilated cardiomyopathy: the mechanism of functional mitral regurgitation. Circulation 1983; 68: 498-508.*

22. Kono T, Sabbah HN, Rosman H, Alam M, Jafri S, Stein PD, Goldstein S. *Mechanism of functional mitral regurgitation during acute myocardial ischemia. J Am Coll Cardiol 1992; 19: 1101-5.*

23. Sabbah HN, Kono T, Rosman H, Jafri S, Stein PD, Goldstein S. *Left ventricular shape: a factor in the etiology of functional mitral regurgitation in heart failure. Am Heart J 1992; 123: 961-6.*

24. Ormiston JA, Shah PM, Tei C, Wong M. *Size and motion of the mitral valve annulus in man. I. A two-dimensional echocardiographic method and findings in normal subjects. Circulation 1981; 64: 113-20.*

25. He S, Lemmon JD Jr, Weston MW, Jensen MO, Levine RA, Yoganathan AP. *Mitral valve compensation for annular dilatation: in vitro study into the mechanisms of functional mitral regurgitation with an adjustable annulus model. J Heart Valve Dis 1999; 8: 294-302.*

26. Yiu SF, Enriquez-Sarano M, Tribouilloy C, Seward JB, Tajik AJ. *Determinants of the degree of functional mitral regurgitation in patients with systolic left ventricular dysfunction: A quantitative clinical study. Circulation 2000; 102: 1400-6.*

27. Kwan J, Shiota T, Agler DA, Popovic ZB, Qin JX, Gillinov MA, Stewart WJ, Cosgrove DM, McCarthy PM, Thomas JD. *Geometric differences of the mitral apparatus between ischemic and dilated cardiomyopathy with significant mitral regurgitation: real-time three-dimensional echocardiography study. Circulation 2003; 107: 1135-40.*

28. Kaplan SR, Bashein G, Sheehan FH, Legget ME, Munt B, Li XN, Sivarajan M, Bolson EL, Zeppa M, Arch MZ, Martin RW. *Three-dimensional echocardiographic assessment of annular shape changes in the normal and regurgitant mitral valve. Am Heart J 2000; 139: 378-87.*

29. Kwan J, Qin JX, Popovic ZB, Agler DA, Thomas JD, Shiota T. *Geometric changes of mitral annulus assessed by real-time 3-dimensional echocardiography: becoming enlarged and less nonplanar in the anteroposterior direction during systole in proportion to global left ventricular systolic function. J Am Soc Echocardiogr 2004; 17: 1179-84.*

30. Shiota T, Jones M, Teien DE, Yamada I, Passafini A, Ge S, Sahn DJ. *Dynamic change in mitral regurgitant orifice area: comparison of color Doppler echocardiographic and electromagnetic flowmeter-based methods in a chronic animal model. J Am Coll Cardiol 1995; 26: 528-36.*

31. Shiota T, Jones M, Teien DE, Yamada I, Passafini A, Ge S, Shandas R, Valdes-Cruz LM, Sahn DJ. *Evaluation of mitral regurgitation using a digitally determined color Doppler flow convergence 'centerline' acceleration method. Studies in an animal model with quantified mitral regurgitation. Circulation 1994; 89: 2879-87.*